VPS27 Controls Vacuolar and Endocytic Traffic through a Prevacuolar Compartment in *Saccharomyces cerevisiae*

Robert C. Piper, Antony A. Cooper, Hong Yang, and Tom H. Stevens

Institute of Molecular Biology, University of Oregon, Eugene, Oregon 97403-1229

Abstract. Newly synthesized vacuolar hydrolases such as carboxypeptidase Y (CPY) are sorted from the secretory pathway in the late-Golgi compartment and reach the vacuole after a distinct set of membrane-trafficking steps. Endocytosed proteins are also delivered to the vacuole. It has been proposed that these pathways converge at a "prevacuolar" step before delivery to the vacuole. One group of genes has been described that appears to control both of these pathways. Cells carrying mutations in any one of the class E *VPS* (vacuolar protein sorting) genes accumulate vacuolar, Golgi, and endocytosed proteins in a novel compartment adjacent to the vacuole termed the "class E" compartment, which may represent an exaggerated version of the physiological prevacuolar compartment. We have characterized one of the class E *VPS* genes, *VPS27*, in detail to address this question. Using a temperature-sensitive allele of *VPS27*, we find that upon rapid inactivation of Vps27p function, the Golgi protein Vps10p (the CPY-sorting receptor) and endocytosed Ste3p rapidly accumulate in a class E compartment. Upon restoration of Vps27p function, the Vps10p that had accumulated in the class E compartment could return to the Golgi apparatus and restore correct sorting of CPY. Likewise, Ste3p that had accumulated in the class E compartment en route to the vacuole could progress to the vacuole upon restoration of Vps27p function indicating that the class E compartment can act as a functional intermediate. Because both recycling Golgi proteins and endocytosed proteins rapidly accumulate in a class E compartment upon inactivation of Vps27p, we propose that Vps27p controls membrane traffic through the prevacuolar/endosomal compartment in wild-type cells.

THE biogenesis of the lysosome has provided important insights into the mechanisms of membrane traffic (Kornfeld and Mellman, 1989; Kornfeld, 1992). Much of our knowledge stems from studying the trafficking of the mannose-6-phosphate receptor (M6PR)[1], which sorts a set of hydrolases modified by the addition of mannose-6-phosphate to the lysosome. Two pathways exist by which M6PR can sort hydrolases to the lysosome; one is the uptake of enzymes from the extracellular media via receptor-mediated endocytosis and the other is the sorting of newly synthesized hydrolases from the *trans*-Golgi reticulum/network to the lysosome. These two pathways converge at a stage termed the prelysosomal/late endosomal compartment. Here the lysosomal hydrolase dissociates from the receptor and is ultimately delivered to the lysosome while the receptor recycles to the plasma membrane or *trans*-Golgi reticulum to bind and sort more ligand. Our understanding of this process has been greatly enhanced by the biochemical isolation and characterization of the prelysosomal compartment together with the functional identification of this compartment in cells by monitoring the traffic of newly synthesized proteins and endocytosed proteins en route to the lysosome (Schmid et al., 1988, 1989; Slazman and Maxfield, 1989; Goda et al., 1992). However, little is known about the molecular machinery that controls this critical juncture in post-Golgi membrane traffic.

Like the lysosome of mammalian cells, the yeast vacuole receives traffic from both the secretory pathway and the endocytic pathway, and is the major site of protein degradation afforded by the high concentration of active vacuolar hydrolases (Raymond et al., 1992*b*). Vacuolar hydrolases such as carboxypeptidase Y (CPY) are diverted from the secretory pathway at a step near the late-Golgi compartment and are delivered to the vacuole (Graham and Emr, 1991). Over 50 nonessential genes required for the correct delivery of CPY from the Golgi apparatus to the vacuole have now been identified based on genetic screens that select for yeast strains that secrete CPY (Bankaitis et al., 1986; Rothman et al., 1989; Klionsky et al., 1990; Ray-

Address all correspondence to Tom H. Stevens, Institute of Molecular Biology, University of Oregon, Eugene, OR 97403-1229. Tel.: (503) 346-5884. Fax: (503) 346-4854. E-mail: stevens@molbio.uoregon.edu

1. *Abbreviations used in this paper*: aa, amino acid; CPY, carboxypeptidase Y; HA, hemagglutinin; M6PR, mannose-6-phosphate receptor; *vps*, vacuolar protein sorting; Vps27p, Vps27 protein; YEPD, yeast extract/peptone/dextrose medium.

mond et al., 1992*a*,*b*). One of these genes, *VPS10*, encodes a type I membrane protein that functions as the CPY sorting receptor (Preston et al., 1991; Van Dyck et al., 1992; Marcusson et al., 1994). In analogy with the M6PR in mammalian cells, Vps10p is proposed to bind proCPY in the late-Golgi compartment and deliver this hydrolase to a prevacuolar compartment. The targeting signal on proCPY is provided in the pro region of the enzyme, which is minimally defined by the amino acids QRPL (Valls et al., 1990). Delivery of proCPY to this prevacuolar compartment would allow dissociation of the receptor and ligand and result in the ultimate delivery of proCPY to the vacuole where it is proteolytically cleaved to the mature form. Once CPY is delivered to a prevacuolar compartment, the CPY receptor could then return to the Golgi apparatus to sort more CPY. Although the exact identity and trafficking dynamics through such an intermediate prevacuolar compartment remain obscure, fractionation studies following the trafficking of newly synthesized CPY have identified an intermediate compartment that functionally lies between the Golgi complex and the vacuole (Vida et al., 1993). Complete isolation, characterization, and immunolocalization of the prevacuolar compartment has yet to be achieved. Likewise, the molecular mechanisms that control the formation of this compartment and the flux through it remain obscure.

One insight into this process has been provided by a comprehensive morphological characterization of the *vps* mutants (Raymond et al., 1992*a*). Mutations in a subset of 13 *VPS* genes, categorized as class E *VPS* genes, cause the accumulation of both vacuolar proteins and Golgi proteins into one to two large (0.1–0.2 μm) compartments adjacent to the vacuole (Raymond et al., 1992*a*). Because this novel compartment, hereby referred to as the "class E" compartment, contains high concentrations of both vacuolar proteins and Golgi proteins, it has been hypothesized that the class E compartment may represent an exaggerated version of the physiological prevacuolar compartment. More recently, the **a**-factor receptor (Ste3p), a marker of the yeast endocytic system, has been found to accumulate in similar class E compartments in cells carrying mutations in another class E *VPS* gene, *REN1/VPS2* (Davis et al., 1993). These data suggest that the endocytic and vacuolar biogenesis pathways converge at a step that may be represented by the class E compartment found in mutant cells. The implication from these studies is that the class E *VPS* genes act together at a distinct step along the vacuolar biogenesis pathway to regulate membrane traffic through this prevacuolar compartment.

It is unknown whether the class E compartment itself represents a true intermediate along the vacuolar biogenesis pathway or merely an aberrant compartment that idiosyncratically accumulates post-Golgi/endocytic membrane traffic since previous studies used class E *VPS* null mutants. To characterize the machinery responsible for the generation of the class E compartment, we have cloned one of the class E genes, *VPS27*. We have also constructed temperature-sensitive alleles of *VPS27* that have allowed us to follow the CPY sorting defect and the morphological effects resulting from rapid inactivation and restoration of Vps27 protein (Vps27p) function. We find that inactivation of Vps27p led to the accumulation of both Golgi and endocytic proteins within a class E–like compartment concomitant with the loss of CPY sorting. Furthermore, proteins that had been trapped in the class E–like compartment could rapidly redistribute to the vacuole or recycle to the Golgi complex once Vps27p function was restored. These data demonstrate that the class E compartment represents a physiological intermediate step along the biogenesis pathway between the Golgi apparatus and the vacuole and may provide a genetic and biochemical means to examine this process in detail.

Materials and Methods

Materials

Enzymes used in DNA manipulations were from New England Biolabs

Table I. Yeast Strains Used in this Study

Strain	Genotype	Source
SF838-9D	*MATα pep4-3 leu2-3,112, ura3-52 his4-519 gal2*	Rothman et al., 1989
RPY10	*MATα leu2-3,112 ura3-52 his4-519 gal2*	Piper et al., 1994
AACY5	*MATα vps27Δ::LEU2 leu2-3,112 ura3-52 his4-519 gal2*	This study
HYY1	*MATα vps27Δ::LEU2 pep4-3 leu2-3,112 ura3-52 his4-519 gal2*	This study
RPY2	*MATα vps27-123(ts) leu2-3,112 ura3-52 his4-519 gal2*	This study
RPY3	*MATα vps27-123 (ts) pep4-3 leu2-3,112 ura3-52 his4-519 gal2*	This study
JHRY20-2C	*MATa leu2-3,112 ura3-52 his3-Δ200 can1*	Rothman and Stevens, 1986
HYY2	*MATa VPS27::URA3 leu2-3,112 ura3-52 his3-Δ200 can1*	This study
HYY3	*MATa/α VPS27::URA3/vps27-5 leu2-3,112/leu2-3,112 ura3-52/ura3-52 his3-Δ200/HIS3 HIS4/his4-519 GAL2/gal2 can1/CAN1*	This study
MY1150	*MATa vps23-9 (vpl 15-9) pep4-3 leu2-3,112 ura3-52 his4-519 gal2*	Raymond et al., 1992*a*
MY1885	*MATa vps27-59 (vpl23-5) pep4-3 leu2-3,112 ura3-52 his4-519 gal2*	Raymond et al., 1992*a*
RPY32	*MATα vps10Δ::URA3 leu2-3,112 ura2-52 his4-519 gal2*	This study
MY1668	*MATa vps23-18 (vpl 15-18) his4 leu2 lys2 ura3 pep4-3*	Raymond et al., 1992*a*
MY1653	*MATa vps28-13 (vpl13-11) his4 leu2 lys2 ura3 pep4-3*	Raymond et al., 1992*a*
MY435	*MATa vps7-2 (vpl7-2) his4 leu2 lys2 ura3 pep4-3*	Raymond et al., 1992*a*
MY1044	*MATa vps36-2 (vpl11-2) his4 leu2 lys2 ura3 pep4-3*	Raymond et al., 1992*a*
MY1848	*MATa vps45-1 (vpl28-1) his4 leu2 lys2 ura3 pep4-3*	Raymond et al., 1992*a*
M366	*MATa vps1-4 (vpl1-4) his4 leu2 lys2 ura3 pep4-3*	Raymond et al., 1992*a*
MY1406	*MATa vps26 (vpt4) ade2 his3 leu2 suc2 trp1 ura3*	Robinson et al., 1988

HYY2 is congenic to JHRY20-2C. All RPY strains in this table are congenic to SF838-9D.

(Beverly, MA), Boehringer Mannheim Biochemicals (Indianapolis, IN), Bethesda Research Laboratories (Gaithersburg, MD), or United States Biochemical Corp. (Cleveland, OH). Goat-α-rabbit and goat-α-mouse alkaline phosphatase conjugates used for CPY overlay blots were purchased from Promega Corp. (Madison, WI). The ECL kit from Amersham Corp. (Arlington Heights, IL) was used in conjunction with HRP-conjugated antibodies for the development of immunoblots. Secondary antibodies used for indirect immunofluorescence experiments (all cross-species adsorbed) were purchased from Jackson Immunoresearch Laboratories Inc. (West Grove, PA). Fixed *Staphylococcus aureus* cells (Ig sorb) were obtained from The Enzyme Center (Malden, MA). [^{35}S]-Express label was from New England Nuclear (Boston, MA). Oxlyticase was from Enzogenetics (Corvallis, OR). The CBZ Phe-F_3Leu was obtained as described previously (Raymond et al., 1990). All other reagents were purchased from Sigma Chemical Co. (St. Louis, MO).

Cloning of VPS27

VPS27 was cloned by complementation of the CPY secretion defect of the MY1885 strain carrying the *vps27-5* (*vpl23-5*) allele. The MY1885 strain was transformed with a multicopy YEp24-based genomic library (Carlson and Botstein, 1982). To select for plasmids that complemented the CPY sorting defect, Ura$^+$ transformants were grown on plates containing the negative selection compound CBZ-Phe-F_3Leu (Raymond et al., 1990). Large colonies were then screened for their ability to correctly sort CPY using a previously described CPY overlay blot technique (Roberts et al., 1991). One of the complementing plasmids, pVPL23-1, was further analyzed by Tn10 transposon tagging analysis according to the procedures of Huisman et al. (1987). Briefly, pVPL23-1 was transformed in the *Escherichia coli* strain DB1329 that was subsequently infected with bacteriophage λLUK containing the Kan^R gene. Plasmids were prepared from pooled kanamycin-resistant colonies and transformed into MY1885 cells. Plasmids were rescued from Ura$^+$ transformants that secreted CPY and mapped to locate the minimal complementing region.

The cloned insert was genetically mapped in yeast by integration of plasmid pCKR230 linearized at the NcoI site into the JHRY20-2C to produce the Leu$^+$ HYY2 strain. The HYY2 strain was then crossed with the MY1885 (*vps27-5*) strain. The resulting diploid (HYY3) was sporulated and dissected. Tetrad analysis of the sporulated diploids showed that all were parental ditypes for the Leu and Vps phenotypes, confirming that the cloned DNA fragment had integrated at the *VPS27* locus.

Strains, Growth of Cells, and Construction of Plasmids

DNA manipulations and DNA-mediated transformation of *E. coli* strain MC1061 were performed by routine procedures. Sequencing of both strands of the 3,230-bp BamHI/EcoRI–complementing region of *VPS27* (These sequence data are available from Genbank under accession number U24218) was completed by sequencing plasmids derived from pHY2 and pHY3 generated using the Erase-a-base kit as specified by the manufacturer (Promega Corp.). PCR amplifications were performed with Vent polymerase (New England Biolabs).

The plasmid pHY1 was generated by subcloning the complementing 3,230-bp BamHI/EcoRI fragment of *VPS27* into pRS316. The plasmid pHY2 was generated by subcloning the 3,230-bp BamHI/EcoRI fragment of *VPS27* into pBluescriptSK$^+$. The plasmid pKJH1 was generated by subcloning the same BamHI/EcoRI fragment into pUC19. The plasmid pHY3 was made by subcloning the SalI/EcoRI fragment of pKJH1 into pBluescriptSK$^+$. The integrating plasmid, pCKR230, was made by subcloning the 1.5-kb BamHI/XbaI fragment of pHY1 into the *LEU2*-containing plasmid pRS305 (Sikorski and Hieter, 1989). The *vps27Δ* plasmid, pKJH2, the 1.2-kb BglII/ClaI fragment of pKJH1 was replaced with the *LEU2* gene derived as a 2-kb HpaI/HpaI fragment (Raymond et al., 1992*a*).

The HA epitope was inserted into *VPS27* by first removing the BamHI site from pHY3 by blunt end ligation of the BamHI site, generated by cutting with BamHI and filling in with Klenow to yield pHY8. A BamHI site was inserted into the 3′ end of the *VPS27* ORF just before the stop codon by in vitro mutagenesis of pHY8 using the oligonucleotide GCTAATAGAGCTTGGATCCATAATATTGTAGC and using the bacterial strain CJ236 and the helper phage KO7 according to the method of Kunkel (Kunkel et al., 1987). The resulting plasmid, pHY10, was used to subclone a BglII linker (encoding three copies of the HA epitope: YPYDVPDYA) into the BamHI site to yield pRCP1. The EcoRI/SalI fragment of pRCP1 was subcloned into the EcoRI/SalI sites of pRS316 to yield pRCP4.

To construct alleles of *VPS27* that contained mutations at the codons predicted to coordinate the binding of zinc, pHY2 was subjected to Kunkel mutagenesis using the following oligonucleotides: $Cys_{176}(C_1)$ GATTCTGATGCGGCCATGATTTGCTCG; and $Cys_{222}(C_7)$ GCCAGTCAGAGTGGCCGATAGCTGC. The BamHI/EcoRI of resulting plasmids pRCP25 and pRCP27, respectively, were subcloned into pRS316 to yield pRCP28 and pRCP34. Mutagenesis of $His_{203}(H_6)$ and $Cys_{179}(C_2)$ was performed by Kunkel mutagenesis with pHY1 resulting in the plasmids pRCP30 and pRCP32 respectively, using the oligonucleotides: $His_{203}(H_6)$ GATTTCTGCCAAGAAGCGAGTTCAAATAGTATACCC; $Cys_{179}(C_2)$ GATGCTTGTATGATCGCGAGTAAAAAGTTTTCT. The mutagenized region of all of these plasmids was confirmed by DNA sequencing.

Expression of yeast protein fragments in bacteria was done by using pEXP1 and pEXP2 (Roberts et al., 1989). The bacterial production of Vps27p polypeptides was done by subcloning both the 771-bp SpeI/XbaI fragment of the *VPS27* gene (amino acids [aa] 16–273) into the SpeI/XbaI sites of pEXP1 produce pCKR124 and by subcloning the 939-bp SpeI/HindIII fragment from the *VPS27* gene (aa 16–311) into the SmaI/HindIII sites of pEXP1 to produce pCKR128. The bacterial expression plasmid for fragments of Vps10p (*PEP1*; these sequence data are available from Genbank under accession number Z34098) were produced by subcloning the 1.2-kb DraI–SpeI fragment of the *VPS10* gene (aa 306–696) into the SmaI/XbaI sites of pEXP2-S to yield pAAC208. A second bacterial expression plasmid for Vps10p was made by subcloning the DraI/SpeI fragment of *VPS10* into the plasmid pMAL in frame with the maltose-binding protein (New England Biolabs) to produce pAAC209. The 2μ plasmid

Table II. Plasmids Used in this Study

Plasmid	Description	Source
pVPL23-1	plasmid from YEp24 library containing *VPS27*	This study
pHY1	3,230-bp BamHI/EcoRI fragment of *VPS27* into pRS316	This study
pHY2	3,230-bp BamHI/EcoRI fragment of *VPS27* into pBluescriptSK$^+$	This study
pKJH1	3,230-bp BamHI/EcoRI fragment into pUC19	This study
pHY3	SalI/EcoRI fragment of pKJH1 into pBluescriptSK$^+$	This study
pCKR230	1.5-kb BamHI/XbaI fragment of pHY1 into the integrating plasmid pRS305	This study
pKJH2	1.2-kb BglII/ClaI fragment of pKJH1 was replaced with the *LEU2* gene	Raymond et al., 1992*a*
pRCP4	HA epitope–tagged *VPS27* in pRS316	This study
pRCP28	$Cys_{176}(C_1)$ to Ala mutation of *VPS27* in pRS316	This study
pRCP32	$Cys_{179}(C_2)$ to Ala mutation of *VPS27* in pRS316	This study
pRCP30	$His_{203}(H_6)$ to Ala mutation of VPS27 in pRS316	This study
pRCP34	$Cys_{222}(C_7)$ to Ala mutation of VPS27 in pRS316	This study
pCKR124	SpeI/XbaI fragment of *VPS27* (aa 16–273) into the SpeI/XbaI sites of pEXP1	This study
pCKR128	SpeI/HindIII fragment of *VPS27* (aa 16–311) into the SmaI/HindIII sites of pEXP1	This study
pSL2015	c-*myc*–tagged *STE3* under the control of *GAL1* promoter in pRS316	Davis et al., 1993
pKE50	HpaI/PvuII fragment of *VPS10* into SmaI site of the 2μ plasmid YEp352	This study
pAAC208	DraI/SpeI fragment of *VPS10* into SmaI/XbaI sites of pEXP2-S expression plasmid	This study
pAAC209	DraI/SpeI fragment of *VPS10* into XmnI/XbaI sites of pMAL fusion protein expression plasmid	This study

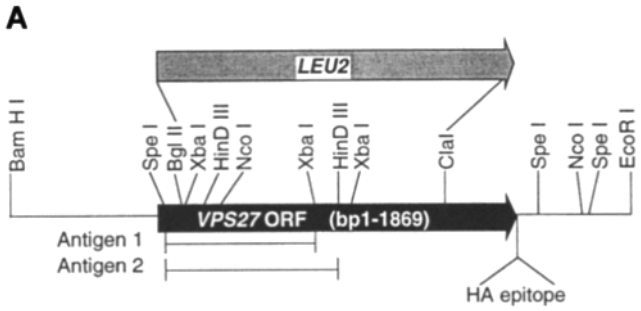

B

```
MSVSTPSELDALIEQATSESIPNGDLDLPIALEISDVLRS      40
RRVNPKDSMRCIKKRILNTADNPNTQLSSWKLTNICVKNG      80
GTPFIKEICSREFMDTMEHVILREDSNEELSELVKTILYE     120
LYVAFKNDSQLNYVAKVYDKLISRGIKFPEKLTLSNSPTA     160
MFDSKTPADWIDSDACMICSKKFSLLNRKHHCRSCGGVFC     200
QEHSSNSIPLPDLGIYEPVRVCDSCFEDYDLKRHDDSKKS     240
KKHRHKRKKDRDYSTPEDEEELIRKAIELSLKESRNSASS     280
EPIVPVVESKNEVKRQEIEEEEDPDLKAAIQESLREAEEA     320
NVRSERQKASRQMQPQQPSPQPQPIHSVDLSDEEKDSIYM     360
FASLVEKMKSRPLNEILEDSKLQNLAQRVFASKARLNYAL     400
NDKAQKYNTLIEMNGKISEIMNIYDRLLEQQLQSINLSQQ     440
YTLPQVPSDPYNYLTENVQNPAESYQTPPLQQLSSHQYKP     480
QQDVSRQQSVKANSSPTTNIDHLKTIDVTPHAQQKPQSHV     520
ELAPSDPPYPKEEAEDEGTQAVQDEESSTQESRERPYPVE     560
TENGETSINKRPQGITRYDFPTVPARKFVQPESTVPLPAS     600
SSEIPIKEERPPSPQEELLIEL.                      623
```

C

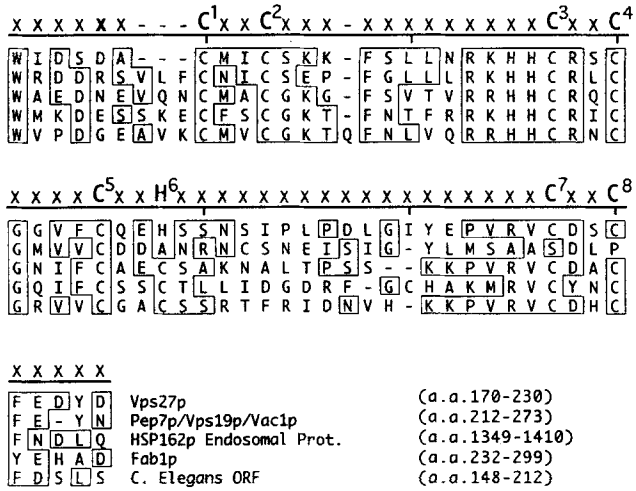

Figure 1. Schematic map of the *VPS27* gene. (*A*) Restriction map of the 3,230-bp BamHI/EcoRI genomic fragment encoding *VPS27* (these sequence data are available from Genbank under accession number U24218). This region was also identified by the genome sequencing project as open reading frame N2038 on the right arm of chromosome XIV (these sequence data are available from Genbank under accession number X77395). The black arrow depicts the *VPS27* open reading frame. The SpeI/XbaI and the SpeI/HindIII fragments (Antigen 1 and Antigen 2, respectively) were expressed in *E. coli* and used in the generation of affinity-purified anti-Vps27p antisera. The HA epitope was inserted at the 3′ end of the open reading frame immediately before the stop codon. The *vps27Δ::LEU2* disruption construct is shown. (*B*) Amino acid sequence of Vps27p. The bold region designates the Zn finger region of Vps27p that is compared in C. (*C*) Sequence comparison of Vps27p with four other proteins that align within the putative Zinc finger region: Pep7p/Vps19p/Vac1p (these sequence data are available from Genbank under accession number M80596); HSP162, *Homo sapiens* protein 162 kD (Genbank accession number X78998); Fab1p (Genbank accession number U01017); *Caenorhabditis elegans* ORF (Genbank accession number U13070). The Cys/His residues predicted to coordinate the binding of Zn are designated C_1 (Cys_{176}), C_2 (Cys_{179}), C_3 (Cys_{192}), C_4 (Cys_{195}), C_5 (Cys_{200}), H_6 (His_{203}), C_7 (Cys_{222}), C_8 (Cys_{225}).

used to overexpress Vps10p was made by subcloning the HpaI/PvuII fragment of *VPS10* into the SmaI site of YEp352 (Hill et al., 1986) to produce pKE50.

Strains were constructed by standard genetic techniques and grown at 30°C in rich media (1% yeast extract, 1% peptone, 2% dextrose; YEPD) or standard minimal medium with appropriate supplements. The HYY1 (*vps27Δ pep4-3*) and AACY5 strain (*vps27Δ PEP4*) was made by transforming SF383-9D and RPY10, respectively, with the *vps27Δ::LEU2* disruption cassette (BamHI/EcoRI fragment) from the plasmid pCKR203 and screening Leu^+ transformants for the secretion of CPY.

Temperature-sensitive mutations in *VPS27* were obtained by subjecting pHY1 to hydroxylamine mutagenesis (0.36 M hydroxylamine for 1 h at 75°C) as previously described (Schauer et al., 1985). Hydroxylamine-treated plasmid DNA was amplified by transformation into MC1061 *E. coli*. The plasmid library was then transformed into the HYY1 strain (*vps27Δ*). Transformants were screened for temperature-sensitive CPY secretion by performing colony blot analyses. The 23 plasmids that conferred correct sorting of CPY at 23°C and secretion of CPY at 37°C were rescued from these transformants and constitute alleles *vps27-100* through *vps27-123*. The insert from plasmid pRCP13, carrying the *vps27-123* allele, was subcloned into the integrating *URA3*-containing vector pRS306 to yield pRCP20. pRCP20 was linearized with BclI and transformed into SF838-9D. The RPY3 strain (*vps27-ts pep4-3*) carrying the stably integrated *vps27-123* allele (*vps27-ts*) was obtained after excision of the endogenous *VPS27* gene by selection on 5-fluoroorotic acid using the two-step gene replacement technique (Boeke et al., 1984).

Immunoprecipitation of ^{35}S-labeled CPY

Secretion of newly synthesized CPY was quantified by immunoprecipitation as previously described (Piper et al., 1994). Briefly, yeast cultures were grown overnight in selective synthetic media without methionine to OD_{600} = 1, centrifuged, and resuspended at OD_{600} = 1 in SD-met/50 mM potassium phosphate, pH 5.7, containing 2 mg/ml BSA. 0.5 OD_{600} of cells were pulse labeled for 10 min with 100 μCi [^{35}S]-Express label and chased for 40 min upon addition of unlabeled methionine and cysteine to a final concentration of 100 μg/ml. The chase was terminated by the addition of sodium azide to 10 mM at 0°C. Cells were separated from the culture media by centrifugation and then spheroplasted. CPY was immunoprecipitated from the resulting intracellular (spheroplasts) and extracellular (media supernatant) fractions and analyzed by SDS-PAGE and fluorography (Stevens et al., 1982). Radioactivity was quantified using a radioanalytic imaging system (AMBIS Systems, Inc., San Diego, CA). To measure the onset of CPY secretion in the RPY3 strain (*vps27-ts*) upon shift to the nonpermissive temperature, cells were grown as above at 23°C. Cell cultures were then shifted to 37°C for various times before the addition of label. To measure the reversal of CPY secretion phenotype after return to the permissive temperature, parallel cultures of RPY3 cells (0.5 OD_{600}) were shifted to 37°C for 25 min and then shifted back to 22°C by the addition of 15°C media (250 μl) and allowed to incubate for various times before the initiation of pulse/chase analysis.

Antibodies and Immunoblotting

Rabbit polyclonal antibodies were generated to fragments of Vps27p that were produced by the *E. coli* strain MC1061 transformed with pCKR124 and purified by SDS-PAGE. The pCKR124-derived Vps27p peptide is designated Antigen 1 (aa 16–273). A second Vps27-derived peptide (Antigen 2; aa 16–311) was produced in MC1061 cells transformed with pCKR128 and purified by SDS-PAGE as previously described (Roberts et al., 1989). This protein was coupled to cyanogen bromide–activated sepharose that

was subsequently used to produce affinity-purified anti-Vps27p antisera as previously described (Raymond et al., 1990).

Antibodies to Vps10p/Pep1p were generated against a bacterial fusion protein produced from plasmid pAAC208. The antisera was affinity purified against a maltose-binding protein fusion that was produced from plasmid pAAC209.

Monoclonal antibodies to the c-*myc* epitope were purified from culture supernatants of hybridoma 9E10 obtained from the American Type Culture Collection (Rockville, MD). Antibodies to the 100-kD V_o subunit of the V-ATPase (Hill and Stevens, 1994) were generated as previously described. The anti-CPY mAb (10A5-B5) and the anti–60-kD subunit of the V-ATPase (13D11-B2) were obtained from Molecular Probes, Inc. (Eugene, OR). The anti-HA mAb was purchased from BAbCO (Richmond, CA).

SDS-PAGE using 10% polyacrylamide gels was performed under reducing conditions according to the method of Laemmli (Laemmli, 1970). Electroblotting was as described (Towbin et al., 1979). Immunoblotting with the anti-Vps27p antibody was done as previously described except that 1% Tween-20 was present during incubations (Rothman and Stevens, 1986).

Fluorescence Microscopy and Image Processing

Indirect immunofluorescence microscopy was performed as previously described (Pringle et al., 1989; Roberts et al., 1991). The anti–c-*myc* and the anti-HA mAbs were used at a final concentration of 10 μg/ml. Cells were photographed using a fluorescent microscope (Axioplan; Carl Zeiss, Inc., Thornwood, NY) and photographed with film (T-MAX 400; Eastman Kodak Co., Rochester, NY).

Immunofluorescence micrographs and autoradiograms were digitized with a flatbed scanner (Reli 4816; Relisys, Milpitas, CA). Images within the same experiment were processed with Adobe Photoshop™ using identical settings and printed on a dye-sublimation printer (Phaser 440; Tektronix, Beaverton, OR).

Temperature-sensitive Experiments

To assess the morphological redistribution of Vps10p, RPY3 cells were grown overnight in YEPD at 22°C after which an aliquot was fixed. The remainder of the cells were warmed to 37°C by the addition of prewarmed YEPD. Cells were incubated at 37°C and samples were removed at various times and fixed at 37°C. After 25 min at the nonpermissive temperature, the culture was divided and cycloheximide was added to one culture to a final concentration of 100 μg/ml. Both cultures were then cooled to 22°C by the addition of chilled YEPD and incubated at 22°C. Samples were removed at various times and fixed at 22°C (Roberts et al., 1991).

To assess the morphological redistribution of Ste3p, RPY3 cells were transformed with plasmid pSL2015 (Davis et al., 1993) carrying the galactose-inducible allele *STE3-c-myc*. Parallel cultures were grown in synthetic media containing 2% raffinose at 22°C overnight. Galactose was added to a final concentration of 2% for 1 h. During this time a negligible amount of Ste3p-c-myc was produced as assessed by immunofluorescence and by immunoblot analysis. Cultures were then shifted to 37°C for 2 h. Cells were pelleted and one culture was resuspended in YEPD and maintained at 37°C and another culture was resuspended in YEPD and maintained at 22°C. Samples were removed and fixed at the respective temperatures at 30 and 60 min after the initiation of the glucose chase. A parallel control culture was maintained at 22°C throughout the 3-h galactose induction and the glucose chase.

Results

Cloning and Characterization of VPS27

The *vps27* mutant was isolated by selecting for mutations in *S. cerevisiae* that result in the missorting and secretion of the vacuolar hydrolase CPY (Rothman and Stevens, 1986; Raymond et al., 1992*b*). To clone the *VPS27* gene, the MY1885 strain bearing the *vps27-5* allele was transformed with a genomic library carried in a 2μ multicopy vector (Carlson and Botstein, 1982). Transformants were grown on plates containing CBZ-Phe-F_3Leu, which inhibits the growth of cells that secrete CPY (Raymond et al., 1990). Transformants were then screened directly for the secretion of CPY by overlay immunoblot analysis using anti-CPY polyclonal antibodies (Roberts et al., 1991). Plasmids that conferred correct sorting of CPY were recovered and the complementing region mapped by subcloning and retransformation into the *vps27* strain (MY1885). The minimal complementing region was encompassed by a 3,230-bp BamHI/EcoRI fragment (Fig. 1). To confirm that the genomic DNA cloned was *VPS27*, a 1.5-kb BamHI/XbaI fragment was subcloned into an integrating vector containing the *LEU2* gene and transformed into the JHRY20-2C strain after linearizing the plasmid by restriction enzyme digestion within the *VPS27* fragment. A Leu^+ transformant (HYY2) was then crossed to the MY1885 strain (*vps27-5*). Tetrad analysis of the resulting diploid (HYY3) showed that all spores from 20 tetrads were parental ditypes (Leu^+ Vps^+ and Leu^- Vps^-) indicating tight linkage between *VPS27::LEU2* and the *vps27-5* allele.

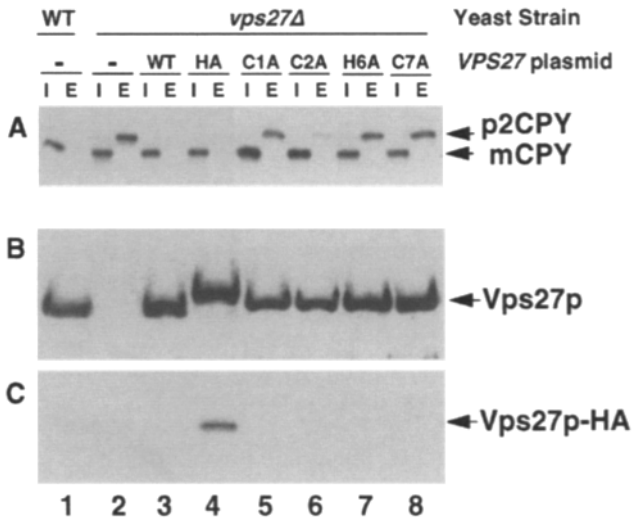

Figure 2. CPY secretion of *vps27Δ* cells. Wild-type cells (RPY10; transformant 1) and *vps27Δ* cells (AACY5; transformants 2–8) were transformed with vector alone (pRS316; 1 and 2); *VPS27* on a centromere-based plasmid (pHY1; 3); HA epitope–tagged *VPS27* on centromere-based plasmid (pRCP4; 4); or mutant *vps27* alleles carrying alanine substitutions at Cys176 (C_1A; 5); Cys179 (C_2A; 6); His203 (H_6A; 7); Cys222 (C_7A; 8) carried on the centromere-based plasmids, pRCP28, pRCP34, pRCP30, and pRCP32, respectively. (*A*) The secretion of newly synthesized CPY was measured by metabolically labeling the above transformants with ^{35}S-Express for 10 min and chasing for 40 min at 30°C. CPY was immunoprecipitated from intracellular (*I*) and extracellular (*E*) fractions and analyzed by SDS-PAGE and fluorography. (*B*) Whole-cell extracts of the above transformants were analyzed by immunoblot using polyclonal antibodies specific for Vps27p, or (*C*) anti-HA antibodies. Vps27p migrated with an apparent molecular mass of ~89 kD. (*C*) Whole-cell extracts were also immunoblotted with anti-HA mAbs. The Vps27p-HA migrated with an apparent molecular mass of ~89 kD.

Both strands of the minimal complementing BamHI/EcoRI fragment encompassing the *VPS27* gene were sequenced. This region was also recently identified by the yeast genome project and is reported as ORF N2038 located on the right arm of chromosome XIV (Verhasselt et al., 1994). Analysis of the predicted primary amino acid se-

quence showed that Vps27p is a hydrophilic protein of 621 amino acids (molecular mass 70.9 kD) that contains two putative Zinc finger domains defined by $CX_2C\text{-}X_{12}\text{-}CX_2C$ X_4 $CX_2H\text{-}X_{18}\text{-}CX_2C$. A BLAST search with the *VPS27* open reading frame revealed that Vps27p has limited homology with other proteins implicated in the control of *trans*-Golgi/endocytic traffic. These include Fab1p, a PI(4)P kinase homologue essential for vacuole morphology in *S. cerevisiae* (Yamamoto et al., 1995); Pep7p/Vps19p, a protein required for vacuolar protein sorting and vacuolar inheritance also in *S. cerevisiae* (Weisman and Wickner, 1992; Zhang et al., 1994), and *Homo sapiens* protein 170, a 170-kD protein localized to endosomes of HeLa cells (Fig. 1 *B*). Curiously, the similarity among these proteins is restricted to the putative Zinc finger region. The composition of this type of Zinc finger region is similar to the class of Zinc finger structures that specify protein/protein interactions rather than DNA binding (Berg, 1990; Coleman, 1992). The homology within this region with other proteins involved in post-Golgi membrane traffic implies that this region may represent a discrete functional domain.

The requirement of Vps27p function for CPY sorting was investigated by constructing haploid strains that were disrupted for *VPS27* (*vps27Δ*). This was accomplished by using a plasmid (pKJH2) in which the BglII/ClaI fragment (encompassing amino acids 38–506) of the *VPS27* gene was replaced with the *LEU2* gene (Fig. 1 *C*) (Raymond et al., 1992*a*). Disruption of the *VPS27* locus was confirmed by both immunoblot analysis with antisera raised against the Vps27 protein and by PCR amplification of genomic DNA. We then measured the secretion of newly synthesized CPY by immunoprecipitation (Fig. 2 *A*). Cells were labeled with [^{35}S]-methionine for 7 min and chased with an excess of cold methionine and cysteine for 40 min at 30°C. Labeled CPY was then immunoprecipitated from the intracellular and extracellular fractions and analyzed by SDS-PAGE. Wild-type cells (RPY10) were able to correctly sort CPY to the vacuole and proteolytically process CPY to the mature form. However, cells carrying the *vps27Δ* allele (AACY5) secreted ~50% of newly synthesized CPY in the unprocessed pro form (p2CPY), while the remaining intracellular portion of CPY was fully processed to the mature form indicating that the intracellular CPY had been delivered to a compartment containing active vacuolar hydrolases. There was no secretion defect in AACY5 cells (*vps27Δ*) that had been transformed with the *VPS27* gene carried on a centromere-based plasmid (plasmid pHY1).

Protein extracts from wild-type yeast were analyzed by SDS-PAGE and immunoblot procedures using polyclonal antisera raised against Vps27p. These antibodies specifically recognized a ~85-kD band corresponding to the *VPS27* gene product in both wild-type cells (RPY10) and

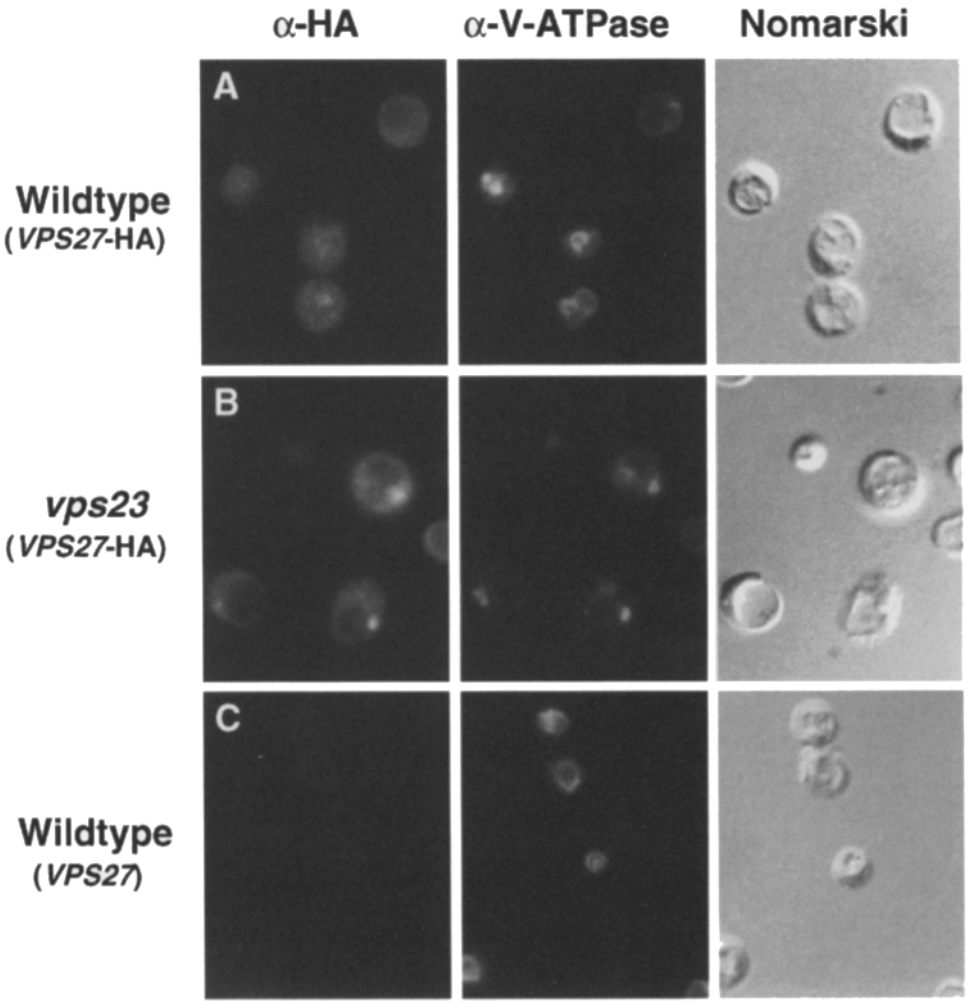

Figure 3. Localization of Vps27p in wild-type and Class E *vps* mutant cells. A centromere-based plasmid carrying an HA-tagged *VPS27* gene (pRCP4) was transformed into wild-type cells (SF838-9D) (*A*) and *vps23* cells (MY1150) (*B*) carrying a mutation in a class E *VPS* gene. Cells were labeled with anti-HA monoclonal antibodies in combination with biotin-linked secondary and streptavidin FITC and also labeled with antibodies to the 100-kD subunit of the V-ATPase in combination with Texas red–conjugated secondary antibodies. The Nomarski image is also shown. As a control for labeling with the anti-HA monoclonal antibodies, wild-type (SF838-9D) cells were transformed with vector alone (pRS316) and labeled as above (*C*).

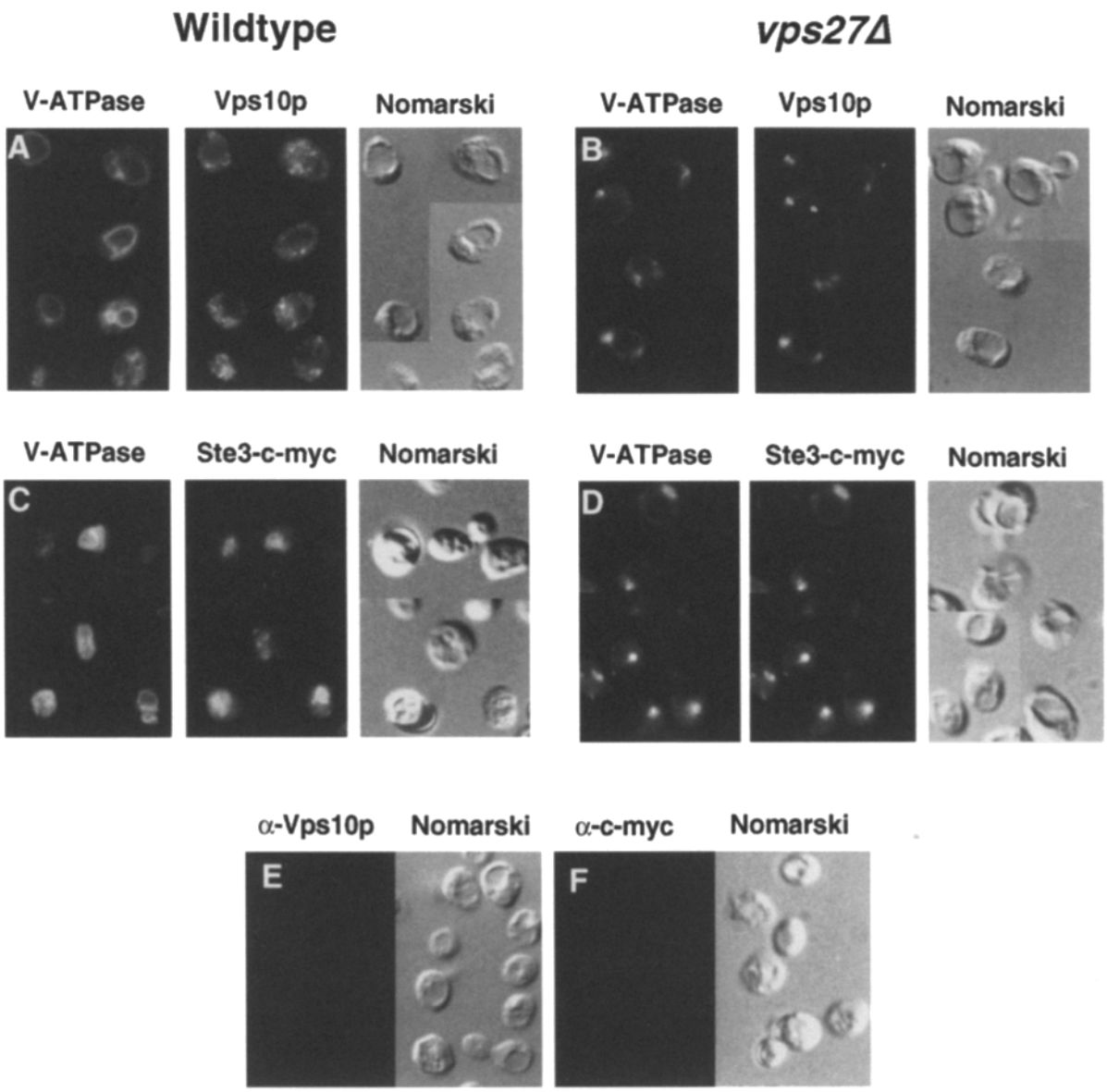

Figure 4. *vps27Δ* cells accumulate Golgi, vacuolar, and endocytosed proteins in the same distinct perivacuolar compartments. Wild-type cells (SF838-9D; left panels *A* and *C*) and *vps27Δ* cells (HYY1; right panels *B* and *D*) were grown overnight in YEPD at 30°C, fixed and spheroplasted, and double labeled with the indicated antibodies. Vps10p was labeled with affinity-purified rabbit polyclonal antibodies in combination with biotin-linked secondary antibody and streptavidin FITC (*A* and *B*). For the localization of Ste3p, wild-type cells (*C*) and *vps27Δ* cells (*D*) were transformed with pSL2015 (*GAL1-STE3-c-myc*) to express c-*myc* epitope–tagged Ste3p. Transformants were grown in galactose for 4 h at 30°C and shifted to glucose-containing media for 30 min before fixation and labeling with anti–c-*myc* monoclonal antibodies. The anti c-*myc* monoclonal antibodies were used to visualize the Ste3p-c-myc in combination with biotin–conjugated secondary antibody and streptavidin FITC. The monoclonal antibodies to the 60-kD V-ATPase subunit (*C* and *D*) and polyclonal antibodies to the 100-kD V-ATPase subunit (*A* and *B*) were visualized by secondary antibody conjugated to Texas red. Labeling of *vps10Δ* cells (RPY32) lacking Vps10p with the Vps10p antibodies (*E*) and labeling of wild-type cells transformed with pRS316 with anti-c-*myc* monoclonal antibodies (*F*) are shown to demonstrate the specificity of immunolabeling.

vps27Δ cells (AACY5) transformed with the *VPS27* plasmid (pHY1), but was absent in *vps27Δ* cells (AACY5) transformed with vector alone (Fig. 2 *B*). No other bands were observed with the anti-Vps27p antisera.

To test whether the putative zinc finger region of Vps27p was required for function, we constructed alleles of *VPS27* with alterations in the residues predicted to coordinate the binding of Zinc. Replacement of either $Cys_{176}(C_1)$, $Cys_{179}(C_2)$, $His_{203}(H_6)$ or $Cys_{222}(C_8)$ of Vps27p with alanine resulted in loss of Vps27p function as shown by a loss in CPY sorting ability (Fig. 2 *A*). The CPY sorting defect of cells carrying the His_{203} (H_6) to Ala allele was greatly exacerbated when cells were grown at 37°C (data not shown). Immunoblot analysis of the cells carrying the mutated Zinc finger residue mutations showed that the Vps27 proteins were stable and produced to similar levels (Fig. 2 *B*).

Fractionation studies were performed to further biochemically characterize Vps27p. We found that ~60% of the Vps27p in whole-cell lysates sedimented with the

membrane fraction, however, this membrane association was only found in the presence of divalent cations. In the presence of EDTA, Vps27p was quantitatively recovered in the cytosolic fractions. Upon further experimentation, we found that the divalent cation–dependent membrane association of Vps27p was independent of mutations in the Zinc finger domain (data not shown).

Vps27p Localizes to the Class E Compartment

We immunolocalized Vps27p to address where Vps27p functions in the vacuolar biogenesis pathway (Fig. 3). To facilitate the localization of Vps27p, we constructed an epitope-tagged allele of *VPS27* by inserting an epitope from the hemagglutinin envelope glycoprotein into the 3′ end of the coding region. The *VPS27-HA* allele was able to fully complement the CPY-secretion defect when introduced into *vps27Δ* cells (AACY5) (Fig. 2 *A*). Immunoblot analysis showed that the epitope-tagged Vps27p (Vps27p-HA) was produced to similar levels as endogenous Vps27p and as expected had an apparent molecular mass of ~4 kD larger than the wild-type Vps27p (Fig. 2 *B*). Vps27p-HA was recognized as a single band by anti-HA monoclonal antibodies (Fig. 2 *C*).

In wild-type cells (SF838-9D), Vps27p-HA was localized to small punctate structures often near the vacuole as well as dispersed throughout the cytoplasm. These structures were distinct from the vacuole as demonstrated by double-label immunofluorescence with antibodies to the 100-kD V-ATPase subunit (Fig. 3 *A*). We next localized Vps27p in cells carrying a mutation in the another class E *VPS* gene, *VPS23*, to determine if the class E compartment itself was the site of Vps27p function. As previously reported for *vps27* and *vps23* mutants, the 100-kD subunit of the V-ATPase accumulates in the class E compartment characterized as 1–3 perivacuolar compartments per cell and thus serves as a good marker for this structure (Raymond et al., 1992*a*). In *vps23* cells (MY1150), Vps27p-HA was localized to 1–3 perivacuolar class E structures (Fig. 3 *B*). These same class E structures also contained the majority of the 100-kD V-ATPase subunit. Wild-type cells not expressing the HA epitope–tagged Vps27p are shown in Fig. 3 *C* as a control for nonspecific labeling. These data imply that Vps27p associates with membranes and that the class E compartment, or physiological counterpart thereof, may be the site of action of Vps27p.

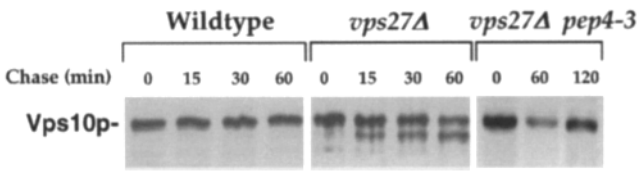

Figure 5. Mislocalization of Vps10p results in its rapid *PEP4*-dependent proteolysis. Vps10p is cleaved in a *PEP4*-dependent manner in *vps27Δ* cells. Wild-type cells (RPY10), *vps27Δ PEP4* cells (AACY5) and *vps27Δ pep4-3* cells (HYY1) were labeled with ^{35}S-Express for 10 min and chased for the times indicated. Labeled Vps10p was immunoprecipitated and analyzed by SDS-PAGE and fluorography.

Vps10p and Ste3p Accumulate in the Class E Compartment

A series of indirect double immunofluorescence labeling experiments were performed to localize markers of the vacuole (V-ATPase), the endocytic system (Ste3p), and the late-Golgi compartment (Vps10p) in both wild-type cells (SF838-9D) and cells disrupted for *vps27Δ* (HYY1) (Fig. 4). Both strains were deficient in vacuolar hydrolases (*pep4-3*) to facilitate the localization of these proteins. The Vps10p membrane protein, a type I membrane protein that functions as the CPY sorting receptor (Marcusson et al., 1994), was immunolocalized using antibodies generated against the large NH_2-terminal luminal domain. In wild-type cells, anti-Vps10p antisera produced a specific Golgi-like labeling pattern composed of 7–12 punctate structures per cell (Fig. 4 *A*). However, in *vps27Δ* cells (HYY1) Vps10p and the V-ATPase were localized to the

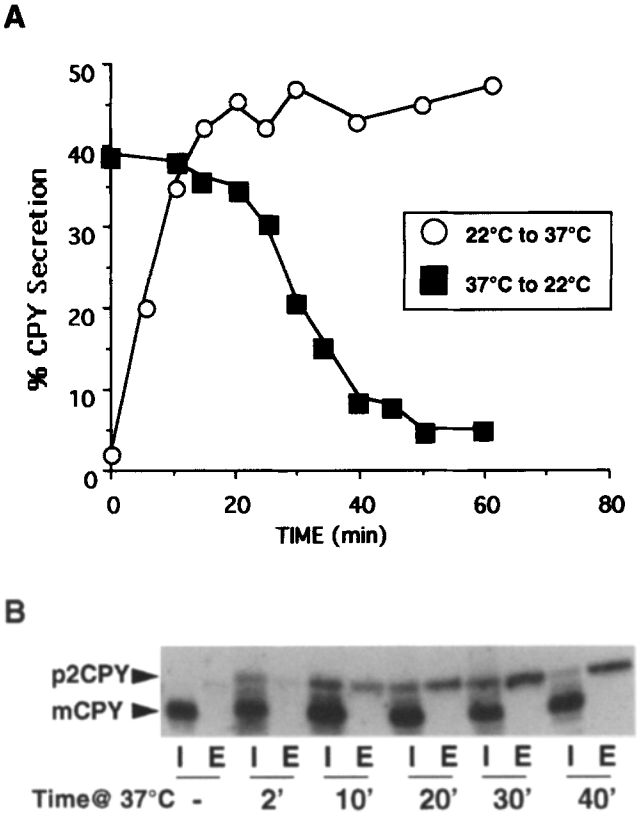

Figure 6. Kinetics of onset and reversal of CPY secretion phenotype in *vps27-ts* cells. The time course of secretion of newly synthesized CPY was measured in *vps27-ts* cells (RPY3) (*open circles*) (*A*). Cells were grown at 23°C and incubated at 37°C for the times indicated before initiation of a 7-min pulse with ^{35}S-Express label and a 35-min chase. CPY was immunoprecipitated from both intracellular and extracellular fractions and the percent of secretion was quantified and plotted as a function of time. The reversal of the CPY-secretion phenotype was measured in RPY3 cells that were shifted to 37°C for 25 min before return to 22°C for the times indicated (*closed squares*). (*B*) Newly synthesized CPY was labeled and immunoprecipitated as above. Immunoprecipitation of CPY from intracellular and extracellular fractions is shown for *vps27-ts* cells (RPY2) preincubated for the indicated times at 37°C before the initiation of a 7-min pulse and 35-min chase.

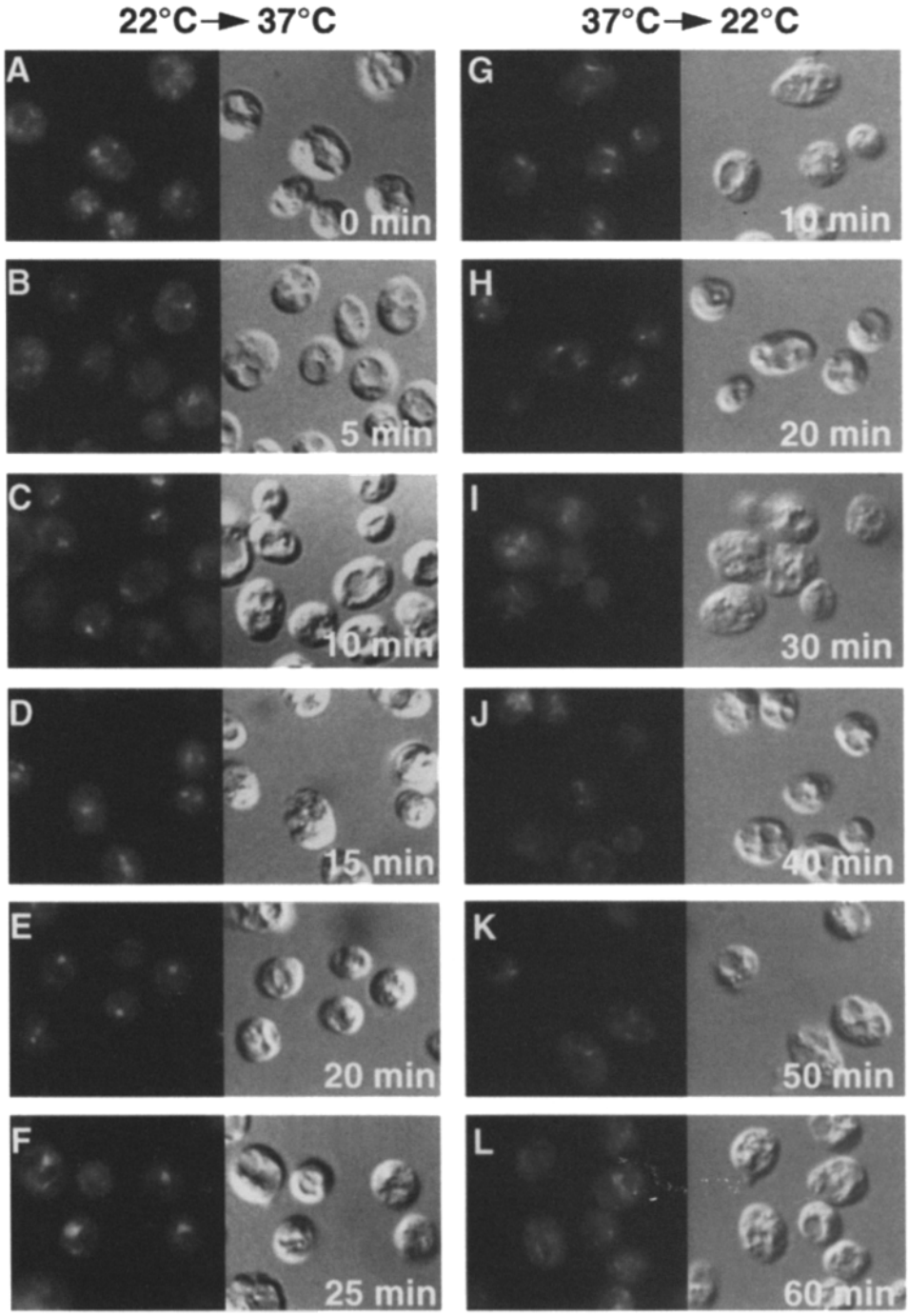

Figure 7. Redistribution of Vps10p in *vps27-ts* cells. *vps27-ts* cells (RPY3) were grown in YEPD at 22°C and shifted to 37°C. Aliquots were removed and fixed at the times indicated (*A–F*). After 25 min at 37°C, cells were shifted back to 22°C and aliquots were removed and fixed at the times indicated (*G–L*). Fixed cells were spheroplasted and labeled with anti-Vps10p antibodies in combination with biotin-linked secondary antibody and streptavidin-conjugated FITC.

same class E structure (Fig. 4 *A*). Morphometric analysis showed that of the cells labeled for both antigens, >95% exhibited colocalization of these antigens. Analysis of the intracellular distribution of these cells showed that although the relative intensities of the staining pattern differed, most of the structures labeled with anti–V-ATPase antibodies were also labeled with anti-Vps10p.

To localize Ste3p we used a c-*myc* epitope–tagged allele of *STE3* under the inducible control of the *GAL1* promoter in both wild-type cells (SF838-9D) and *vps27Δ* cells (HYY1) (Davis et al., 1993). In wild-type cells, Ste3p is rapidly delivered to the vacuole via endocytosis after reaching the plasma membrane (Davis et al., 1993). Cells were grown in galactose for 4 h and then transferred to glucose-containing media before fixation and immunolabeling with anti–c-*myc* monoclonal antibodies. Ste3p was found exclusively in the vacuole of wild-type cells (Fig. 4 *B*); however, in HYY1 cells (*vps27Δ*), Ste3p was localized to the same class E compartments that contained the V-ATPase (Fig. 4 *B*). Thus, the class E compartment present in cells containing the *vps27Δ* allele accumulates traffic from both the vacuolar biogenesis and the endocytic routes.

To examine further the trafficking of Vps10p, we exploited the observation that the class E compartment contains active vacuolar proteases (Raymond et al., 1992*a*). Delivery of Vps10p to a compartment containing vacuolar

hydrolases can be monitored by a *PEP4*-dependent cleavage of the Vps10p luminal domain. This cleavage is observed in cells expressing Vps10p lacking its cytoplasmic Golgi-retention signal or in *vps1Δ* cells expressing wild-type Vps10p (Cooper, A. A., and T. H. Stevens, unpublished observations) since *vps1Δ* cells are defective in Golgi retention and mislocalize Golgi proteins to the vacuole (Wilsbach and Payne, 1993; Nothwehr et al., 1995). We followed the *PEP4*-dependent cleavage of newly synthesized Vps10p in cells lacking Vps27p function. Wild-type cells (RPY10) and *vps27Δ* cells (AACY5) were biosythetically labeled with [^{35}S]methionine for 10 min and then chased in the presence of unlabeled methionine for 15, 30, or 60 min before immunoprecipitation of Vps10p. Fig. 5 shows that in wild-type cells, Vps10p is a very stable protein. However, in *vps27Δ* cells, newly synthesized Vps10p is rapidly cleaved in a *PEP4*-dependent manner indicating delivery to the proteolytically active class E compartment. The half time of proteolytic processing of newly synthesized Vps10p was ~40–50 min.

Rapid Inactivation of Vps27p Leads to Redistribution of the CPY Receptor into the Class E Compartment

As shown in Fig. 4, *vps27Δ* cells accumulate both Vps10p and Ste3p in aberrant class E compartments characteristically close to the vacuole. To address whether the class E compartment observed in cells disrupted for *VPS27* represents a physiological intermediate along the vacuolar biogenesis pathway, we isolated alleles of *VPS27* that were temperature sensitive for function. A library of hydroxylamine-mutagenized centromere-based plasmids containing *VPS27* (plasmid pHY1) was transformed into vps27Δ cells (HYY1). Plasmids were rescued from transformants that secreted CPY when grown at 37°C but not at 22°C. Several temperature-sensitive *vps27* alleles were found and one, *vps27-123*, was found to exhibit ~50% CPY secretion at 37°C and little secretion (~5%) at 22°C. This level of CPY secretion was the same as found in *vps27Δ* cells. The *vps27-123* (*vps27-ts*) allele was integrated at the *VPS27* locus of SF838-9D cells to produce the RPY3 strain (*vps27-ts*).

The onset of the CPY secretion phenotype of *vps27-ts* cells was measured by shifting cells from 22°C to the nonpermissive temperature (37°C) for various times and immunoprecipitating newly synthesized CPY from intracellular and extracellular fractions prepared from [^{35}S]methionine–labeled cells. Half-maximal CPY secretion was observed after 10 min at 37°C demonstrating that there is a rapid loss of Vps27p function upon shift to the nonpermissive temperature (Fig. 6 *A*). Because the onset of CPY secretion was rapid, these data imply that Vps27p plays a direct role in the sorting of CPY. The fate of the remaining intracellular CPY was also monitored at various times after shift to the nonpermissive temperature in *vps27-ts* cells (Fig. 6 *B*). Soon after shift to the nonpermissive temperature a portion of the intracellular CPY is found in the Golgi-modified precursor form (p2 CPY). When cells were maintained for longer times at the nonpermissive temperature before labeling, most of the intracellular CPY was matured, similar to what was observed for *vps27Δ* cells. The most likely explanation is that CPY is delivered to the newly accumulated prevacuole compartment that rapidly becomes proteolytically charged. As the time at the nonpermissive temperature continues, more of the intracellular CPY is processed to the mature form.

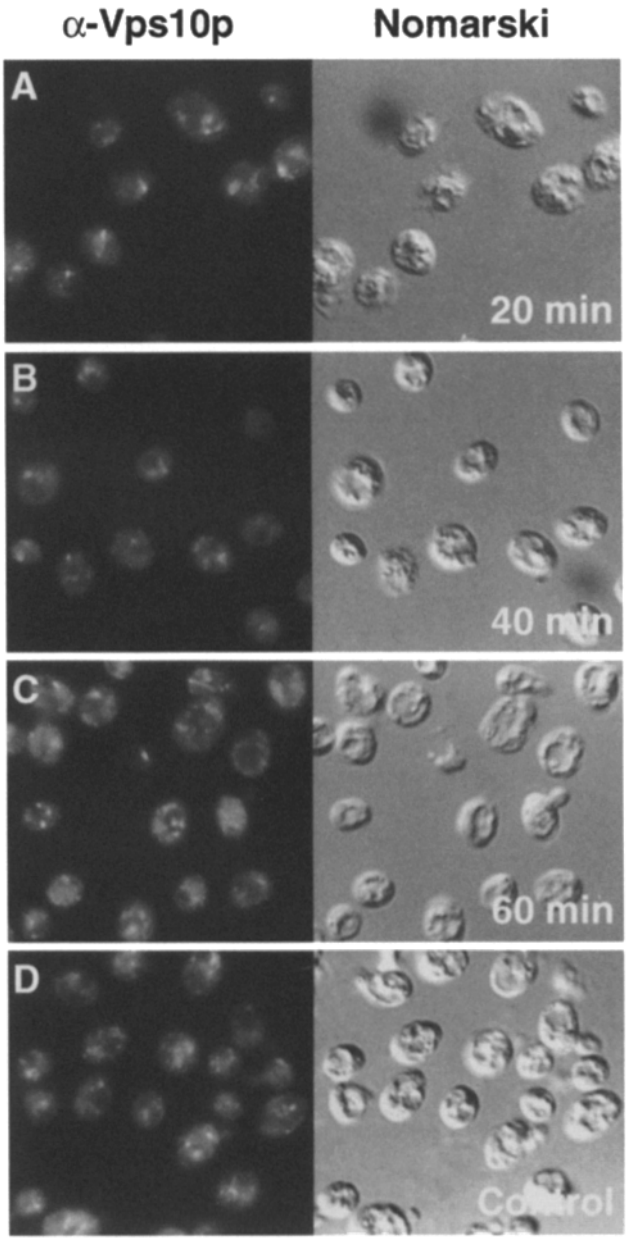

Figure 8. Redistribution of Vps10p in *vps27-ts* cells does not require new protein synthesis. Cells were shifted to 37°C for 25 min as in Fig. 7 except that cells were returned to 22°C in the presence of 100 μg/ml cycloheximide to prevent synthesis of new Vps10p. Aliquots were removed at the times indicated and fixed, spheroplasted, and immunolabeled for Vps10p.

We then investigated the morphological effects of rapid inactivation of Vps27p function. For this analysis we followed the trafficking of the CPY receptor, Vps10p, in cells carrying the *vps27-ts* allele (RPY3). *vps27-ts* cells (RPY3) were grown at 22°C and shifted to 37°C for various times before fixation and immunolabeling with anti-Vps10p antibodies (Fig. 7). In *vps27-ts* cells grown at 22°C, Vps10p

was distributed in 7–12 punctate structures and was indistinguishable from the labeling pattern observed in wild-type cells grown either at 30 (Fig. 3), 22, or 37°C (data not shown). Upon shift to 37°C, Vps10p rapidly redistributed from a punctate pattern to one to three perivacuolar structures very similar to the class E compartments observed in *vps27Δ* cells (HYY1) (Fig. 4). Partial redistribution of Vps10p was observed as early as 5 min at the nonpermissive temperature. Redistribution of Vps10p to class E structures was maximal by 25 min at 37°C and no further effects on Vps10p distribution were observed in cells maintained at 37°C for 2 h (data not shown). Morphometic analysis of immunofluorescence images revealed that by 20 min 91% of the *vps27-ts* cells showed a class E–like phenotype, with most of the Vps10p localized in one to two perivacuolar compartments. In contrast, only 3% of *vps27-ts* cells maintained at 22°C displayed a class E–like morphology. The kinetics of the morphological redistribution of Vps10p to class E–like structures (Fig. 7) closely followed the onset of the CPY secretion phenotype (Fig. 6).

The rapid accumulation of Vps10p into class E structures coupled with the simultaneous loss of CPY sorting is consistent with the model that Vps27p controls the flux through a compartment through which Vps10p normally passes. To test further whether the class E compartment that accumulates after loss of Vps27p function represents a physiologically relevant prevacuolar compartment, we determined whether Vps10p could redistribute from the class E compartment back to its wild-type punctate distribution once Vps27p function was restored. *vps27-ts* cells (RPY3) were grown at 22°C and shifted to 37°C for 25 min to accumulate Vps10p into class E structures, and then shifted back to 22°C for various times before fixation and immunolabeling with anti-Vps10p antibodies (Fig. 7). Redistribution of Vps10p from the class E structures to a wild-type punctate distribution was evident by 30 min at 22°C and complete by 40 min. At intermediate times, Vps10p was often observed in small tubulelike processes emanating from the class E compartment. The redistribution kinetics of Vps10p back to its wild-type pattern closely paralleled the return of CPY sorting function (Fig. 6). Correct sorting of CPY in *vps27-ts* cells (RPY3) was restored by 35 min af-

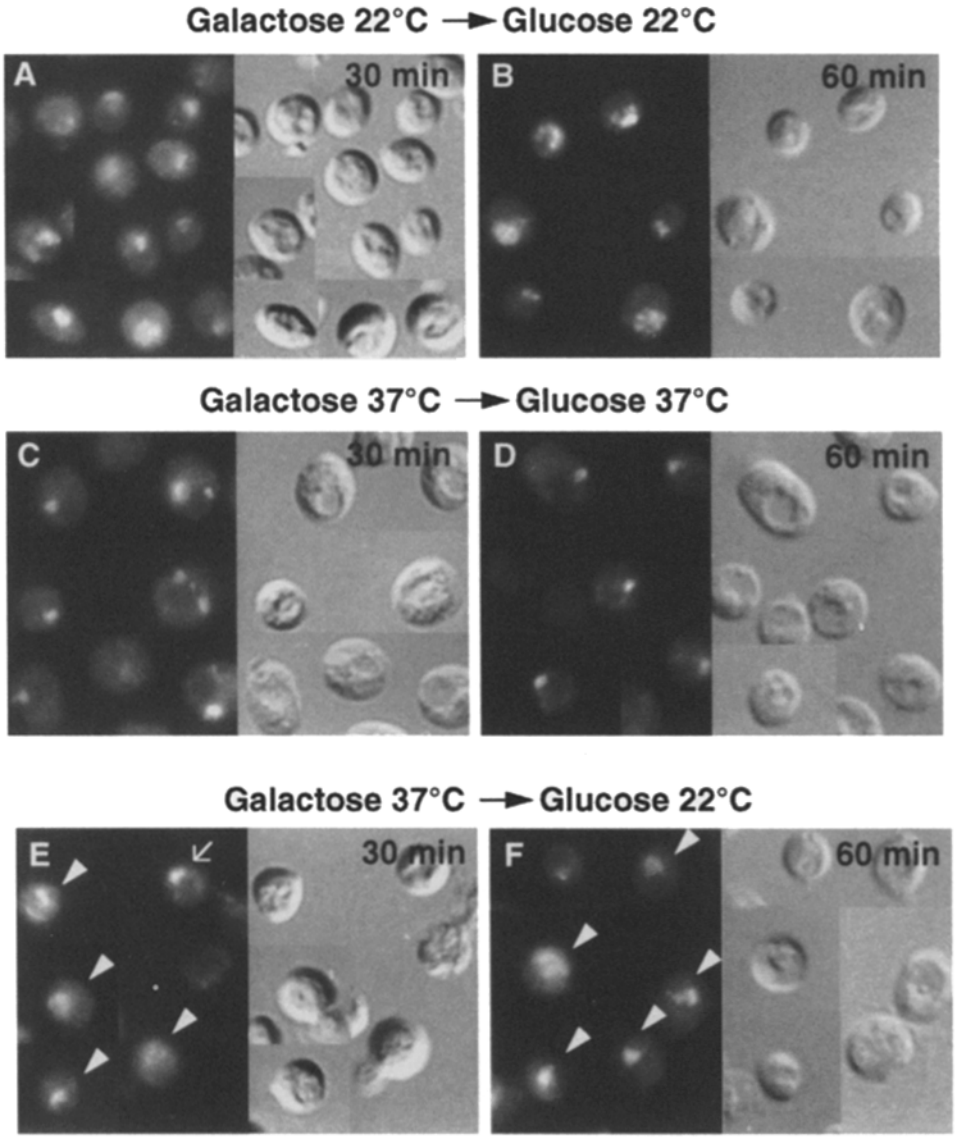

Figure 9. Ste3p is reversibly trapped in the class E compartment in *vps27-ts* cells. *vps27-ts* cells (RPY3) were transformed with the centromere-based plasmid pSL2015 (*GAL1-STE3*-c-myc). Transformants were grown in galactose at either 22°C (*A* and *B*) or 37°C (*C–F*). Cells were then resuspended in glucose-containing media at 22°C (*A* and *B* and *E* and *F*) or 37°C (*C* and *D*). Aliquots were removed and fixed at 30 and 60 min after the addition of glucose and immunolabeled with anti–c-*myc* monoclonal antibodies in combination with biotin-linked secondary antibodies and streptavidin FITC. In *E* and *F*, vacuolar labeling and labeling of the class E compartment are indicated by arrowhead (◄) and arrow (←) respectively.

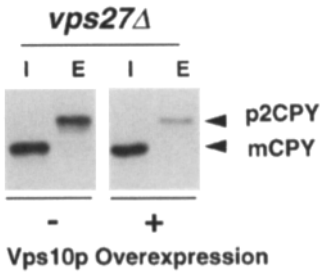

Figure 10. Overexpression of Vps10p can suppress the CPY secretion phenotype of *vps27Δ* cells. *vps27Δ* cells (AACY5) were transformed with a multicopy plasmid carrying *VPS10* (+; pKEY50) or vector alone (−; YEp352). Newly synthesized CPY was immunoprecipitated from intracellular (*I*) and extracellular (*E*) fractions prepared from transformants labeled with ^{35}S-Express for 10 min and chased for 35 min.

ter return to the permissive temperature indicating that Vps10p had functionally redistributed to the Golgi complex where it could bind ligand.

To exclude the possibility that the apparent redistribution of Vps10p upon reversal of the temperature-sensitive block was entirely due to new synthesis of Vps10p, we followed the fate of Vps10p during morphological reversal in the presence of cycloheximide. *vps27-ts* cells (RPY3) were grown at 22°C and shifted to 37°C for 25 min. Cycloheximide was added (100 μg/ml) immediately before shifting cells back to 22°C for various times before fixation and immunolabeling with anti-Vps10p antibodies. Fig. 8 shows that the kinetics of Vps10p redistribution from class E compartment to a punctate wild-type distribution was unaffected by cycloheximide. Cycloheximide had no effect on cells maintained at 22°C (Fig. 8 *D*) and had no effect on the kinetics of Vps10p redistribution to the class E compartment upon shift from 22°C to the nonpermissive 37°C (data not shown). These data indicate that once Vps10p accumulates in the class E compartment it redistributes to the Golgi apparatus in a functional manner and is not delivered to the vacuole for degradation once Vps27p function is restored.

Ste3p Is Transported from the Class E Compartment to the Vacuole Once Vps27p Function Is Restored

Both vacuolar and endocytic traffic accumulates in the class E compartment implying that this compartment may represent an exaggerated version of where both pathways intersect. To test further whether the class E compartment represents an intermediate compartment encountered en route to the vacuole, we determined whether an endocytosed protein (Ste3p) trapped in the class E compartment could progress to the vacuole upon restoration of Vps27p function. We followed the distribution of the **a**-factor receptor (Ste3p) in *vps27-ts* cells (RPY3) carrying a centromere-based plasmid containing a c-myc epitope–tagged allele of *STE3* under the inducible control of the *GAL1* promoter. Thus, Ste3p-c-myc could be induced by the addition of galactose at the nonpermissive temperature (37°C) and its distribution followed after return to the permissive temperature (22°C) in the absence of new synthesis of Ste3p-c-myc afforded by glucose repression. Cells were grown to mid-log phase at 22°C in media containing raffinose; production of the Ste3p was induced by the addition of galactose to cells maintained at 22°C or shifted to 37°C. After the induction of Ste3p-c-myc at 37°C, cells were washed and resuspended in media containing 2% glucose and maintained at either 37°C or shifted to 22°C for both 30 min and 60 min before fixation and immunolabeling with anti–c-*myc* mAbs. New synthesis of Ste3p-c-myc was inhibited by glucose repression of the *GAL1* promoter during the 30- and 60-min chase periods.

Fig. 9 (*A* and *B*) shows that the Ste3p-c-myc protein induced at 22°C was correctly localized to the vacuole in a very similar distribution as reported by Davis et al. (1993). When Ste3p-c-myc synthesis was induced at 37°C and maintained at 37°C in glucose for either 30 or 60 min, Ste3p-c-myc was localized to 1–2 perivacuolar compartments characteristic of class E structures (Fig. 9, *C* and *D*). However, when Ste3p-c-myc was induced at 37°C but followed by a glucose chase at 22°C we found that Ste3p was localized to the vacuole. After 30 min at 22°C, both class E–like structures as well as vacuoles were labeled for Ste3p-c-myc indicating that there was partial delivery of Ste3p-c-myc to the vacuole. The delivery of Ste3p to the vacuole was complete by 60 min after return to the permissive temperature (Fig. 9 *F*). These data show that the endocytosed Ste3p accumulates in the class E compartment in the absence of Vps27p function and can proceed from there to the vacuole once Vps27p function is restored. These data imply that the class E compartment that accumulates in the absence of Vps27p represents a functional intermediate in the endocytic pathway to the vacuole.

Overexpression of Vps10p Suppresses the vps27Δ CPY Sorting Defect

The data presented above indicate that the loss of Vps27p function results in the accumulation of a post-Golgi/prevacuolar compartment that traps membrane traffic along both the endocytic and the vacuolar biogenesis pathways. The concomitant redistribution of the CPY receptor, Vps10p, with the loss of CPY sorting indicates that CPY secretion is caused by depleting the late-Golgi compartment of functional Vps10p. One possible explanation is that the recycling of Vps10p from the class E compartment back to the Golgi apparatus is inhibited. To test this we determined whether overexpression of Vps10p could suppress the CPY sorting defect in *vps27Δ* cells. Overproduction of Vps10p would increase the level of Vps10p in the late-Golgi sorting compartment independent of receptor recycling. Newly synthesized CPY was immunoprecipitated from intracellular and extracellular fractions from *vps27Δ* cells (AACY5) transformed with either a multicopy vector carrying *VPS10* or vector alone. *vps27Δ* cells carrying vector alone secreted ~45% of newly synthesized CPY, whereas *vps27Δ* cells overexpressing Vps10p secreted only ~10% (Fig. 10). Immunoblot analysis of whole-cell extracts of the corresponding cells showed that Vps10p was overproduced by the multicopy plasmid by >10-fold (data not shown). All of the intracellular CPY was processed to the mature form indicative of its delivery to a proteolytically charged class E compartment. These data imply that the binding and sorting of CPY by Vps10p as well as trafficking of Vps10p from the Golgi apparatus to the class E compartment is normal, but that Vps10p fails to recycle to the Golgi complex in the absence of Vps27p function.

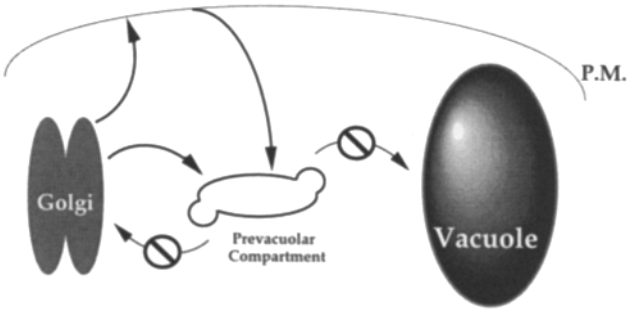

Figure 11. Model of Vps27p function. Delivery of CPY from the late-Golgi sorting compartment to the vacuole is thought to involve a transport intermediate shown as a prevacuolar compartment. This prevacuolar compartment lies within the intersection of the endocytic and vacuolar biogenesis pathways and is presumably the site where p2CPY is uncoupled from the CPY-sorting receptor, Vps10p. Loss of Vps27p may block the return of Golgi proteins from this compartment as well as vacuolar and endocytosed proteins to the vacuole. This block would result in the accumulation of these proteins in an exaggerated compartment that resembles the physiological prevacuolar compartment.

We also surveyed the CPY secretion phenotype in various other *vps* mutants for their ability to be suppressed by overexpression of Vps10p. We observed marked suppression in other class E *vps* mutants (*vps23* and *vps28*) while no suppression was observed in *vps8* (class A) *vps34* (class D), *vps45* (class D) *vps1* (class F), or *vps26* (class F) mutant strains (data not shown). Thus, the ability of CPY secretion to be suppressed by overexpression of Vps10p appears to be a general feature of class E *vps* mutants and not other classes of *vps* mutants.

Discussion

Our initial molecular characterization of *VPS27* was motivated by the observation that mutations in *VPS27* caused the accumulation of both Golgi proteins and vacuolar proteins in a novel compartment adjacent to the vacuole. Mutations in 12 other *VPS* genes result in a very similar phenotype to *vps27Δ* and have been collectively referred to as class E *VPS* genes (Raymond et al., 1992*a*) because of the accumulation of these distinctive class E compartments. One of the class E *vps* mutants, *vps2/ren1*, has also been shown to accumulate the **a**-factor receptor Ste3p in similar class E compartments (Davis et al., 1993). More recently, the lipid-soluble styryl dye FM-464, which serves as an endocytic tracer, has also been shown to accumulate in class E–like structures (Vida and Emr, 1995). Our analysis of *vps27Δ* cells confirms these earlier findings as we show that endocytosed Ste3p, and the CPY sorting receptor, Vps10p, which functions in the late-Golgi compartment, are colocalized within the same distinct class E compartments as the V-ATPase. Other proteins such as the ER membrane protein Dpm1p, and the plasma membrane protein Pma1p, maintain their normal localization in cells carrying the *vps27Δ* allele (data not shown). More importantly, the remainder of the secretory pathway is functionally intact in class E *vps* mutants, since CPY as well as other secretory proteins are secreted as fully Golgi-modified glycoproteins. Thus, the accumulation of membrane traffic in the class E compartment appears to be specific for proteins that move through post-Golgi/endocytic compartments.

The convergence of both the endocytic pathway and the vacuolar pathway within the class E compartment has led to the idea that the class E compartment may represent an exaggerated version of a physiological prevacuolar compartment through which endocytic and Golgi proteins normally pass. Such an exaggerated compartment would result if membrane traffic out of this compartment were inhibited. Alternatively, loss of Vps27p function may indirectly lead to the sequestration of membrane traffic in an entirely aberrant compartment that does not reflect a physiological process. To distinguish between these possibilities, we have constructed temperature-sensitive alleles of *VPS27* and followed the morphological changes upon rapid inactivation of Vps27p function. Our premise was that if the class E compartment results from a block in traffic at a prevacuolar intermediate step through which membrane traffic normally travels, then both Golgi proteins and endocytosed proteins should reversibly accumulate at this step upon inactivation of Vps27p function.

In *vps27-ts* cells we found that the CPY receptor, Vps10p, rapidly accumulated in class E structures upon shift to the nonpermissive temperature. This redistribution of Vps10p was concomitant with the onset of CPY secretion. The CPY secretion defect is most likely due to the depletion of Vps10p from the late-Golgi sorting compartment and its accumulation in a post-Golgi compartment, since overexpression of Vps10p suppressed the CPY secretion defect in cells lacking Vps27p function. Once Vps27p function was restored by returning *vps27-ts* cells to 22°C, we found that Vps10p redistributed from class E compartments back to a dispersed punctate distribution indistinguishable from that observed in wild-type cells. CPY sorting was also restored in concert with the redistribution of Vps10p, indicating that functional Vps10p had reached the Golgi complex. The thermo-reversibility of the class E compartment was also observed for the endocytic marker, Ste3p. Once Ste3p had been trapped in the class E compartment in *vps27-ts* cells at the nonpermissive temperature, Ste3p could progress to the vacuole once Vps27p function was restored. Thus, in both onset and reversal experiments, the class E compartment itself can define an intermediate step between the plasma membrane and the vacuole as well as serve as a site for the recycling of Vps10p back to the Golgi complex.

Our general model for Vps27p function is shown in Fig. 11 and predicts that Vps27p acts at the level of a prevacuolar compartment that serves as a transport intermediate along the vacuolar biogenesis pathway. Such a prevacuolar compartment is analogous to the prelysosomal compartment in mammalian cells that receives lysosomal hydrolases from clathrin-coated vesicles derived from both the plasma membrane and the *trans*-Golgi reticulum (Marquardt et al., 1987; Griffiths et al., 1988). In the delivery of CPY to the vacuole, this prevacuolar compartment would not only serve as the site where the CPY receptor, Vps10p, would dissociate from proCPY and recycle to the Golgi complex, but also where endocytic traffic would travel en route to the vacuole. It is likely that the physiological counterpart

of the class E compartment may itself be the site of intersection between these two pathways. The existence of a prevacuolar compartment is supported by fractionation studies that have kinetically identified a prevacuolar intermediate that contains newly synthesized proCPY and is distinct from the late-Golgi compartment (Vida et al., 1993). Similarly, studies by Singer-Krüger and co-workers have identified distinct endocytic intermediates en route to the vacuole (Singer and Riezman, 1990; Singer-Krüger et al., 1993).

The existence of such a prevacuolar compartment along the vacuolar biogenesis pathway would also predict that at least two distinct vesicle budding/fusion steps may be required for traffic from the Golgi complex to the vacuole. Supporting this prediction is the finding that there are two distinct Rab proteins (Vps21p/Ypt51p and Ypt7p) and Sec1p-like proteins (Vps45p and Vps33p) that have been shown to control vacuolar protein sorting (Banta et al., 1990; Wichmann et al., 1992; Schimmoller and Riezman, 1993; Cowles et al., 1994; Horazdovsky et al., 1994; Piper et al., 1994; Singer-Krüger et al., 1994).

Vps27p, and the other class E Vps proteins, appear to control the flux of protein traffic out of the prevacuolar compartment. Loss of Vps27p function would lead to an accumulation of membrane traffic at this step and lead to the exaggeration of this compartment. This is supported by ultrastructural examination of *vps27-ts* cells after shift to the nonpermissive temperature that shows an aggregation of tubular elements into a distinctive fenestrated structure that is also observed in *vps27Δ* cells (Whitters, E. A., and T. H. Stevens, unpublished observations). Exactly how the loss of Vps27p inhibits the movement of proteins out of the prevacuolar compartment remains to be determined. Vps27p may function in a general way to effect the tubularization or vesiculation of prevacuolar membranes. Alternatively, Vps27p may be required for sorting and segregation of proteins returning to the Golgi complex from those destined for the vacuole within the prevacuolar compartment. Thus, perhaps in the absence of such a sorting step, the prevacuolar compartment may not be able to vesiculate.

Further insights into how the class E Vps proteins function on the molecular level may be provided by the cloning and sequencing of this class of *VPS* genes. One clue as to the mechanism of Vps27p function is provided by the observation that Vps27p itself associates with the class E compartment when localized in cells carrying a mutation in another class E *VPS* gene (Fig. 4). These data imply that Vps27p may act on the prevacuolar compartment itself presumably in concert with a host of other proteins responsible for its membrane association. Given the similarities among their mutant phenotypes, the likely candidates for such interaction are the other class E Vps proteins themselves (Raymond et al., 1992*a*). This will motivate the exploration of biochemical and genetic interactions among the class E *VPS* genes. Furthermore, the ability to rapidly accumulate the class E compartment will also enable biochemical analysis of this elusive compartment and help differentiate distinct transport steps along the vacuolar biogenesis pathway.

We thank Chris Raymond for the initial work on characterization of *VPS27*; Kathryn Hill, Laurie Graham, and Steve Nothwehr for affinity-purified antibodies; Eric Whitters for discussions about the ultrastructure of *vps27Δ* mutants.

This work was supported by postdoctoral fellowships from the American Heart Association to A. A. Cooper and the National Institutes of Health (GM16601-01) to R. C. Piper, and a grant from the National Institutes of Health (GM32448) to T. H. Stevens.

Received for publication 5 May 1995 and in revised form 2 August 1995.

References

Bankaitis, V. A., L. M. Johnson, and S. D. Emr. 1986. Isolation of yeast mutants defective in protein targeting to the vacuole. *Proc. Natl. Acad. Sci. USA.* 83: 9075–9079.

Banta, L. M., T. A. Vida, P. K. Herman, and S. D. Emr. 1990. Characterization of yeast Vps33p, a protein required for vacuolar protein sorting and vacuole biogenesis. *Mol. Cell. Biol.* 10:4638–4649.

Berg, J. M. 1990. Zinc fingers and other metal-binding domains: elements for interactions between macromolecules. *J. Biol. Chem.* 265:6513–6516.

Boeke, J. D., F. LaCroute, and G. R. Fink. 1984. A positive selection for mutants lacking orotidine-5′-phospahte decarboxylase activity in yeast: 5-fluoroorotic acid resistance. *Mol. & Gen. Genet.* 197:345–346.

Carlson, M., and D. Botstein. 1982. Two differentially regulated mRNAs with different 5′ ends encode secreted proteins with intracellular forms of yeast invertase. *Cell.* 28:145–154.

Coleman, J. E. 1992. Zinc proteins: enzymes, storage proteins, transcription factors, and replication proteins. *Annu. Rev. Biochem.* 61:897–946.

Cowles, C. R., S. D. Emr, and B. F. Horazdovsky. 1994. Mutations in the *VPS45* gene, a *SEC1* homologue, result in vacuolar protein sorting defects and accumulation of membrane vesicles. *J. Cell Sci.* 107:3449–3459.

Davis, N. G., J. L. Horecka, and G. F. Sprague, Jr. 1993. *Cis-* and *trans*-acting functions required for endocytosis of the yeast pheromone receptors. *J. Cell Biol.* 122:53–65.

Goda, Y., T. Soldati, and S. R. Pfeffer. 1992. Transport from late endosomes to trans-Golgi network in semiintact cell extracts. *Methods Enzymol.* 219:153–159.

Graham, T. R., and S. D. Emr. 1991. Compartmental organization of Golgi-specific protein modification and vacuolar protein sorting events defined in a yeast *sec18* (*NSF*) mutant. *J. Cell Biol.* 114:207–218.

Griffiths, G., B. Holflack, K. Simons, I. Mellman, and S. Kornfeld. 1988. The mannose-6-phosphate receptor and the biogenesis of lysosomes. *Cell.* 52: 329–341.

Hill, K. J., and T. H. Stevens. 1994. Vma21p is a yeast membrane protein retained in the endoplasmic reticulum by a di-lysine motif and is required for the assembly of the vacuolar H^+-ATPase complex. *Mol. Biol. Cell.* 5:1039–1050.

Hill, J. E., A. M. Myers, T. J. Koerner, and A. Tzagologg. 1986. Yeast/*E. coli* shuttle vectors with multiple unique restriction sites. *Yeast.* 2:163–167.

Horazdovsky, B. F., G. R. Busch, and S. D. Emr. 1994. *VPS21* encodes a rab5-like GTP binding protein that is required for the sorting of yeast vacuolar proteins. *EMBO (Eur. Mol. Biol. Organ.) J.* 13:1297–1309.

Huisman, O., K.-U. Raymond, P. Froehlich, N. Erranda, D. Kleckner, D. Botstein, and M. A. Hoyt. 1987. A Tn10-lacZ-kanR-URA3 gene fusion transposon for insertion mutagenesis and fusion analysis of yeast and bacterial genes. *Genetics.* 116:191–199.

Klionsky, D. J., P. K. Herman, and S. D. Emr. 1990. The fungal vacuole: composition, function, and biogenesis. *Microbiol. Rev.* 54:266–292.

Kornfeld, S. 1992. Structure and function of the mannose 6-phosphate/insulin-like growth factor II receptors. *Annu. Rev. Biochem.* 61:307–330.

Kornfeld, S., and I. Mellman. 1989. The biogenesis of lysosomes. *Annu. Rev. Cell Biol.* 5:483–525.

Kunkel, T. A., J. D. Roberts, and R. A. Zakour. 1987. Rapid and efficient site-specific mutagenesis without phenotypic selection. *Methods Enzymol.* 154: 367–382.

Laemmli, U. K. 1970. Cleavage of structural proteins during the assembly of the head of bacteriophage T4. *Nature (Lond.).* 227:680–685.

Marcusson, E. G., B. F. Horazdovsky, J. L. Cereghino, E. Gharakhanian, and S. D. Emr. 1994. The sorting receptor for yeast vacuolar carboxypeptidase Y is encoded by the *VPS10* gene. *Cell.* 77:579–586.

Marquardt, T., T. Braulke, A. Hasilik, and K. von Figura. 1987. Association of the precursor of cathepsin D with coated membranes. Kinetics and carbohydrate processing. *Eur. J. Biochem.* 168:37–42.

Nothwehr, S. F., E. Conibear, and T. H. Stevens. 1995. Golgi and vacuolar membrane proteins reach the vacuole in *VPS1* mutant yeast cells via the plasma membrane. *J. Cell Biol.* 129:35–46.

Piper, R. C., E. A. Whitters, and T. H. Stevens. 1994. Yeast Vps45p is a Sec1p-like protein required for the consumption of vacuole-targeted, post-Golgi vesicles. *Eur. J. Cell Biol.* 65:305–318.

Preston, R. A., J. D. Garman, L. B. Daniels, and E. W. Jones. 1991. Map positions of *pet9*, *pep1* and *pdr4* with respect to *CEN2*. *Yeast.* 7:857–858.

Pringle, J. R., R. A. Preston, A. E. M. Adams, T. Stearns, D. G. Drubin, B. K. Haarer, and E. W. Jones. 1989. Fluorescence microscopy methods for yeast. *Methods Cell. Biol.* 31:357–435.

Raymond, C. K., P. J. O'Hara, G. Eichinger, J. H. Rothman, and T. H. Stevens. 1990. Molecular analysis of the yeast *VPS3* gene and the role of its product in vacuolar protein sorting and vacuolar segregation during the cell cycle. *J. Cell Biol.* 111:877–892.

Raymond, C. K., I. Howald-Stevenson, C. A. Vater, and T. H. Stevens. 1992*a*. Morphological classification of the yeast vacuolar protein sorting mutants: evidence for a prevacuolar compartment in class E *vps* mutants. *Mol. Biol. Cell.* 3:1389–1402.

Raymond, C. K., C. J. Roberts, K. E. Moore, I. Howald, and T. H. Stevens. 1992*b*. Biogenesis of the vacuole in *Saccharomyces cerevisiae*. *Int. Rev. Cytol.* 139:59–120.

Roberts, C. J., G. Pohlig, J. H. Rothman, and T. H. Stevens. 1989. Structure, biosynthesis, and localization of dipeptidyl aminopeptidase B, an integral membrane glycoprotein of the yeast vacuole. *J. Cell Biol.* 108:1363–1373.

Roberts, C. J., C. K. Raymond, C. T. Yamashiro, and T. H. Stevens. 1991. Methods for studying the yeast vacuole. *Methods Enzymol.* 194:644–661.

Robinson, J. S., D. J. Klionsky, L. M. Banta, and S. D. Emr. 1988. Protein sorting in *Saccharomyces cervisiae*: isolation of mutants defective in the delivery and processing of multiple vacuolar hydrolases. *Mol. Cell. Biol.* 8:4936–4948.

Rothman, J. H., and T. H. Stevens. 1986. Protein sorting in yeast: mutants defective in vacuole biogenesis mislocalize vacuolar proteins into the late secretory pathway. *Cell.* 47:1041–1051.

Rothman, J. H., C. P. Hunter, L. A. Valls, and I. H. Stevens. 1986. Overproduction-induced mislocalization of a yeast vacuolar protein allows isolation of its structural gene. *Proc. Natl. Acad. Sci. USA.* 83:3248–3252.

Rothman, J. H., I. Howald, and T. H. Stevens. 1989. Characterization of genes required for protein sorting and vacuolar function in the yeast *Saccharomyces cerevisiae*. *EMBO (Eur. Mol. Biol. Organ.) J.* 8:2057–2065.

Schauer, I., S. Emr, C. Gross, and R. Schekman. 1985. Invertase signal and mature sequence substitutions that delay intercompartmental transport of active enzyme. *J. Cell Biol.* 100:1664–1675.

Schimmoller, F., and H. Riezman. 1993. Involvement of Ypt7p, a small GTPase, in traffic from late endosome to the vacuole in yeast. *J. Cell Sci.* 106:823–830.

Schmid, S. L., R. Fuchs, P. Male, and I. Mellman. 1988. Two distinct subpopulations of endosomes involved in membrane recycling and transport to lysosomes. *Cell.* 52:73–83.

Schmid, S., R. Fuchs, M. Kielian, A. Helenius, and I. Mellman. 1989. Acidification of endosome subpopulations in wild-type Chinese hamster ovary cells and temperature-sensitive acidification-defective mutants. *J. Cell Biol.* 108: 1291–1300.

Sikorski, R. S., and P. Hieter. 1989. A system of shuttle vectors and yeast host strains designed for efficient manipulation of DNA in *Saccharomyces cerevisiae*. *Genetics.* 122:19–27.

Singer, B., and H. Riezman. 1990. Detection of an intermediate compartment involved in transport of alpha-factor from the plasma membrane to the vacuole in yeast. *J. Cell Biol.* 110:1911–22.

Singer-Krüger, B., R. Frank, F. Crausaz, and H. Riezman. 1993. Partial purification and characterization of early and late endosomes from yeast: identification of four novel proteins. *J. Biol. Chem.* 268:14376–14386.

Singer-Krüger, B., H. Stenmark, A. Dusterhöft, P. Philippsen, J.-S. Yoo, D. Gallwitz, and M. Zerial. 1994. Role of three rab5-like GTPases, Ypt51p, Ypt52p, and Ypt53p, in the endocytic and vacuolar protein sorting pathways of yeast. *J. Cell Biol.* 125:283–298.

Slazman, N. H., and F. R. Maxfield. 1989. Fusion accessibility of endocytic compartments along the recycling and lysosomal endocytic pathways in intact cells. *J. Cell Biol.* 109:2097–2104.

Stevens, T., B. Esmon, and R. Schekman. 1982. Early stages in the yeast secretory pathway are required for transport of carboxypeptidase Y to the vacuole. *Cell.* 30:439–448.

Towbin, H., T. Staehelin, and J. Gordon. 1979. Electrophoretic transfer of proteins from polyacrylamide gels to nitrocellulose sheets: procedure and some applications. *Proc. Natl. Acad. Sci. USA.* 76:4350–4354.

Valls, L. A., J. R. Winther, and T. H. Stevens. 1990. Yeast carboxypeptidase Y vacuolar targeting signal is defined by four propeptide amino acids. *J. Cell Biol.* 111:361–368.

Van Dyck, L., B. Purnelle, J. Skala, and A. Goffeau. 1992. An 11.4 kb DNA segment on the left arm of yeast chromosome II carries the carboxypeptidase Y sorting gene *PEP1*, as well as *ACH1*, *FUS3*, and a putative *ARS*. *Yeast.* 8:769–776.

Verhasselt, P., R. A. Marleen, M. Voet, and G. Volckaert. 1994. Twelve open reading frames revealed in the 23.6 kb segment flanking the centromere on the *Saccharomyces cerevisiae* chromosome XIV right arm. *Yeast.* 10:1355–1361.

Vida, T. A., and S. D. Emr. 1995. A new vital stain for visualizing vacuolar membrane dynamics and endocytosis in yeast. *J. Cell Biol.* 128:779–92.

Vida, T. A., G. Huyer, and S. D. Emr. 1993. Yeast vacuolar proenzymes are sorted in the late Golgi complex and transported to the vacuole via a prevacuolar endosome-like compartment. *J. Cell Biol.* 121:1245–1256.

Weisman, L. S., and W. Wickner. 1992. Molecular characterization of *VAC1*, a gene required for vacuole inheritance and vacuole protein sorting. *J. Biol. Chem.* 267:618–623.

Wichmann, H., L. Hengst, and D. Gallwitz. 1992. Endocytosis in yeast: evidence for the involvement of a small GTP-binding protein (Ypt7p). *Cell.* 71: 1131–1142.

Wilsbach, K., and G. S. Payne. 1993. Vps1p, a member of the dynamin GTPase family, is necessary for Golgi membrane protein retention in *Saccharomyces cerevisiae*. *EMBO (Eur. Mol. Biol. Organ.) J.* 12:3049–3059.

Yamamoto, A., D. B. DeWald, I. V. Bornonenkov, R. A. Anderson, S. D. Emr, and D. Koshland. 1995. Novel PI(4)P 5-kinase homolog, Fab1p, essential for normal vacuole function and morphology in yeast. *Mol. Biol. Cell.* 6:525–539.

Zhang, J.-Q., G. C. Webb, and E. W. Jones. 1994. *PEP7. In* Guide to the Secretory Pathway. J. Rothblatt, P. Novick, and T. Stevens, editors. Oxford University Press, Oxford, UK. 250–251.